Chapter 3

Bounce Averaged Electron Fluid Equations

NEW FLUID EQUATIONS FOR TRAPPED ELECTRONS are developed in this chapter. The fluid equations for the ions derived in Chapter 2 can accurately describe the dynamics of the toroidal ITG and (somewhat less accurately) trapped ion modes when the electrons are adiabatic, but for realistic tokamak parameters, the nonadiabatic electron response, which primarily comes from trapped electrons, is often important. Proper treatment of the nonadiabatic electron response is essential to describe electron heat transport and particle transport. When the electrons are purely adiabatic, there is no net particle transport, since the $\mathbf{E} \times \mathbf{B}$ convection of the perturbed electron density is zero ($\mathbf{E} \times \mathbf{B} \cdot \nabla \tilde{n}_e \propto \nabla \tilde{\Phi} \times \mathbf{B} \cdot \nabla \tilde{\Phi} = 0$). Quasineutrality then implies no net ion transport. In addition, in the adiabatic limit there are no electron temperature fluctuations, so there is no electron heat transport. Trapped electrons are a well known important destabilization mechanism; the drive from the trapped electron toroidal precession resonance can double the growth rate of the ITG mode in some regimes, and can also destabilize the trapped electron mode (TEM). In this chapter, a sophisticated bounce averaged trapped electron fluid model is derived which retains the pitch angle dependence of the trapped electron response, as opposed to more simplified trapped electron models which assume the electrons are deeply trapped [Kadomtsev and Pogutse, 1970]. Retaining this pitch angle dependence is potentially important for advanced tokamak configurations in the second stability regime or with reversed magnetic shear [Kessel *et al.*, 1994], where a major fraction of the trapped electrons have favorable toroidal precession drift. It also allows use of a full pitch angle scattering collision operator for electron collisions (and not a Krook-type algebraic approximation), so these equations are continuously valid from the collisionless regime, where the trapped electron response is driven by the toroidal precession resonance, to the dissipative regime, to the very collisional regime where the trapped electrons become adiabatic.

Since their fast parallel motion allows bounce averaging of the electrons, the fast parallel time scale is removed, and these trapped electron fluid equations are not numerically stiff. Coupled with the ion equations derived in Chapter 2, these equations can be used efficiently in high resolution 3D toroidal simulations which simultaneously include trapped electron effects as well as the ITG drive, and enable calculation of the full transport matrix: electron and ion heat fluxes and particle fluxes.

3.1 Nonlinear Bounce Averaged Kinetic Equation

The electron dynamics are actually simpler than the ion dynamics in two respects, because $m_e \ll m_i$. Firstly, since the turbulent scales are on the order of the ion gyroradius, $k_\perp \rho_e \ll 1$, so we can neglect FLR effects for the electrons and use the drift kinetic equation instead of the gyrokinetic equation. Secondly, the turbulent time scales (on the order of the ion transit frequency, $\omega_{ti} = v_{ti}/qR$, or the diamagnetic frequency, $\omega_* = k_\perp \rho_i v_{ti}/L_n$) are long compared to the electron bounce frequency, $\omega \ll \omega_{be} = v_{te}/qR$. (This ordering breaks down for barely trapped particles, where $\omega_{be} \to 0$, but only over a very small region of velocity space.) Thus we can average over the fast electron bounce motion, so the trapped electron dynamics are described by the nonlinear bounce averaged drift kinetic equation [Gang and Diamond, 1990]:

$$(\frac{\partial}{\partial t} + i\omega_{de} - C)\tilde{h}_n^e = -\frac{e}{T_e}F_e(\frac{\partial}{\partial t} + i\omega_{*e}^T)\left\langle e^{-inq\theta}\Phi_n\right\rangle_b + N_n. \tag{3.1}$$

This equation is four dimensional (two velocity space and two configuration space dimensions), since the variation along the field line has been removed by bounce averaging. Before deriving the trapped electron fluid equations, it is useful to rewrite this equation in a form more suitable for taking moments.

In Eq. (3.1), $\tilde{h}_n^e$ is the nonadiabatic part of the electron distribution function, $f_e = F_e e\Phi/T_e + h_e$. This equation was derived for axisymmetric circular concentric flux surfaces, and the perturbed distribution function and potential were written using:

$$h_e(r,\theta,\zeta) = \sum_n h_n^e(r,\theta)e^{-in\zeta}, \tag{3.2}$$

$$\Phi(r,\theta,\zeta) = \sum_n \Phi_n(r,\theta)e^{-in\zeta}. \tag{3.3}$$

To lowest order in ω/ω_{be}, the fast parallel motion causes h_e to be constant along the field line, so

$$h_n^{e(0)} = \tilde{h}_n^e(r)e^{inq\theta}, \tag{3.4}$$

and h_e is zero to lowest order in ω/ω_{be} for passing electrons. Thus Eq. (3.1) describes the evolution of the bounce averaged part of the nonadiabatic electron distribution function. The bounce average is defined by:

$$\langle A(r,\theta,\zeta)\rangle_b = \frac{\oint dl/|v_\parallel| A(r,\theta,\zeta)}{\oint dl/|v_\parallel|}, \tag{3.5}$$

where the integration is along a field line, and l is the distance along the field line. The nonlinear term N_n describes convection by the bounce averaged $\mathbf{E}\times\mathbf{B}$ drift:

$$N_n = -i\frac{c}{B}\sum_{n_1+n_2=n}\left(\frac{n_2 q}{r}\tilde{h}_{n_2}^e\frac{\partial}{\partial r}\left\langle e^{-in_1 q\theta}\Phi_{n1}\right\rangle_b - \frac{n_1 q}{r}\left\langle e^{-in_2 q\theta}\Phi_{n2}\right\rangle_b\frac{\partial}{\partial r}\tilde{h}_{n_2}^e\right). \tag{3.6}$$

Using a field-aligned coordinate system, as described in Chapter 4, this equation can be cast in a simpler form. Specifically, if we use the transformation Eq. (4.36), where x is the radial variable, y is perpendicular and mostly poloidal, and $z = \theta$ is the coordinate along the field line, we can rewrite Eqs. (3.2) and (3.4):

$$h_e(r,\theta,\zeta) = h_e(x,y,z) = \sum_n \tilde{h}_n^e(r)e^{-in(\zeta-q\theta)} = \sum_{k_y} h_e(x,k_y)e^{ik_y y}, \tag{3.7}$$

so to lowest order in ω/ω_{be}, h_e is independent of the coordinate along the field line, z. At fixed z, the y variable is simply the toroidal angle, so h_e can be thought of as the distribution function of banana centers at minor radius x and toroidal angle y. It will be most convenient to use the velocity space variables v and κ, where v is the total velocity ($E = v^2/2$) and κ is a pitch angle variable defined by:

$$\kappa^2 = \frac{1-\mu B_{\min}/E}{2\epsilon_B}, \tag{3.8}$$

where $\epsilon_B = (B_{\max} - B_{\min})/2B_{\max}$. This is the pitch angle at the outer midplane normalized to unity at the trapped-passing boundary, and is a constant of the electron bounce motion. For deeply trapped electrons (with $E = \mu B_{\min}$), $\kappa = 0$; and the maximum κ for passing particles (where $\mu = 0$) is $1/\sqrt{2\epsilon_B}$. At the trapped-passing boundary (where $E = \mu B_{\max}$), $\kappa = 1$. For trapped particles ($\kappa < 1$), the poloidal angle of the banana tip or turning point, θ_t, is related to κ by:

$$\kappa = \sin(\theta_t/2). \tag{3.9}$$

This can be seen by using $E = \mu B_t$ where B at the turning point is $B_t = B_0/(1 + \epsilon\cos\theta_t)$. If we expand for small $\epsilon = r/R_0$, the definition for κ, Eq. (3.8), becomes:

$$\kappa^2 = [v^2/2 - \mu B_0(1-\epsilon)]/\epsilon v^2. \tag{3.10}$$

This pitch angle variable differs slightly from the one used in [Gang and Diamond, 1990], $\kappa^2 = [v^2/2 - \mu B_0(1-\epsilon)]/2\epsilon\mu B_0$, but for trapped particles the difference is negligible since $v \approx v_\perp$. So to lowest order in ω/ω_{be}, the nonadiabatic distribution function is a function of two spatial coordinates (x and y) and two velocity space coordinates, (v and κ). The eikonal $e^{-inq\theta}$ appears inside the bounce average $\left\langle \Phi_n e^{-inq\theta}\right\rangle_b$ since Eq. (3.1) has been written as an evolution equation for $\tilde{h}_n^e$, and both sides of $(\partial h_e/\partial t + \cdots)$ have been multiplied by $e^{-inq\theta}$. Using Eq. (3.8) to write $|v_\parallel|$ in terms of v and κ: $|v_\parallel| = v\sqrt{1 - B/B_{\min}(1-2\epsilon_B\kappa^2)}$, the bounce time is

$$\tau_b(\kappa) = \oint dl/|v_\parallel| = \frac{qR}{v}\int_{-\theta_t}^{\theta_t} \frac{d\theta}{\sqrt{1 - B/B_{\min}(1-2\epsilon_B\kappa^2)}}, \tag{3.11}$$

and the bounce average becomes:

$$\langle\Phi\rangle_b(x,y,\kappa) = \frac{\oint dz\Phi(x,y,z)/|v_\parallel|}{\oint d\theta/|v_\parallel|} = \frac{qR}{v}\int_{-\theta_t}^{\theta_t} \frac{d\theta\,\Phi(x,y,\theta)}{\tau_b\sqrt{1 - B/B_{\min}(1-2\epsilon_B\kappa^2)}}, \tag{3.12}$$

Bounce averaging turns functions of θ into functions of pitch angle, because of the κ dependence of the turning point, $|v_\parallel|$, and τ_b. Our derivation is correct for general magnetic geometry, but from time to time it is instructive to look at the large aspect ratio (small ϵ) limit to relate to previous work. Using $B = B_0/(1+\epsilon\cos\theta)$ and expanding for small ϵ leads to the more standard form:

$$\langle\Phi\rangle_b = \int_{-\theta_t}^{\theta_t} \frac{d\theta\,\Phi(x,y,\theta)}{\sqrt{\kappa^2 - \sin^2(\theta/2)}\,4K(\kappa^2)}, \tag{3.13}$$

where $K(\kappa^2)$ is the complete elliptic integral of the first kind,

$$K(\kappa^2) = \int_0^1 \frac{dt}{\sqrt{(1-t^2)(1-\kappa^2 t^2)}} = \int_0^{\pi/2} \frac{dt}{\sqrt{1-\kappa^2 \sin^2 t}}. \tag{3.14}$$

The bounce averaged ∇B and curvature drift frequency, ω_{de}, is the toroidal precession frequency. For small ϵ, this is [Kadomtsev and Pogutse, 1966]:

$$\omega_{de} = \frac{cT_e}{eB}\frac{k_y}{R}\frac{v^2}{2v_{te}^2} G(\hat{s}, \kappa), \tag{3.15}$$

$$G(\hat{s}, \kappa) = \left(2\frac{E(\kappa^2)}{K(\kappa^2)} - 1\right) + 4\hat{s}\left(\frac{E(\kappa^2)}{K(\kappa^2)} - 1 + \kappa^2\right),$$

where $E(\kappa^2)$ is the complete elliptic integral of the second kind,

$$E(\kappa^2) = \int_0^1 dt \frac{\sqrt{1-\kappa^2 t^2}}{\sqrt{1-t^2}} = \int_0^{\pi/2} dt \sqrt{1-\kappa^2 \sin^2 t}. \tag{3.16}$$

It is important to keep the pitch angle dependence of ω_{de} to describe the stabilization of trapped electron modes in reversed shear configurations ($\hat{s} < 0$). The limiting values $G(\hat{s}, \kappa = 0) = 1$ and $G(\hat{s}, \kappa = 1) = -1$ are independent of shear, but as $\hat{s}$ decreases, more trapped particles precess in the favorable direction, $G < 0$, as shown in Fig. 3.1.

Finally, ω_{*e}^T is the bounce averaged diamagnetic frequency:

$$\omega_{*e}^T = \frac{cT_e}{eB}\frac{k_y}{L_n}\left[1 + \eta_e\left(\frac{v^2}{v_{te}^2} - \frac{3}{2}\right)\right].$$

To derive electron fluid equations, it is more convenient to write Eq. (3.1) in terms of $\langle f_e \rangle_b$ instead of $\tilde{h}_n^e$. Writing Eq. (3.1) in terms of h_e instead of $\tilde{h}_n^e$ removes the eikonal from inside the bounce average. Then the $\partial/\partial t$ term can be removed from the right hand side of Eq. (3.1) by evolving $\langle f_e \rangle_b$ instead of h_e, using:

$$\langle f_e \rangle_b = \langle h_e \rangle_b (x, y, v, \kappa) + F_e \left\langle \frac{e\Phi}{T_e} \right\rangle_b (x, y, \kappa). \tag{3.17}$$

Since h_e is independent of z to this order in ω/ω_{be}, $\langle h_e \rangle_b = h_e$:

$$f_e = h_e + F_e \frac{e\Phi}{T_e} = \langle h_e \rangle_b + F_e \frac{e\Phi}{T_e} = \langle f_e \rangle_b - F_e \left\langle \frac{e\Phi}{T_e} \right\rangle_b + F_e \frac{e\Phi}{T_e}. \tag{3.18}$$

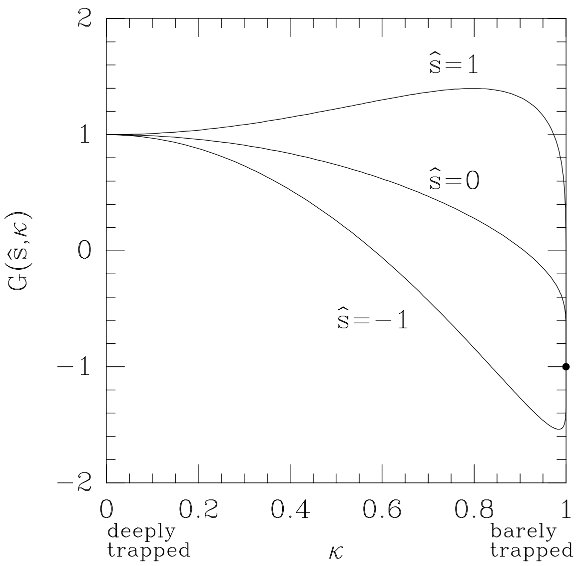

Figure 3.1: Pitch angle dependence of the toroidal precession frequency in the function $G(\hat{s}, \kappa)$.

Then Eq. (3.1) becomes:

$$\left(\frac{d}{dt} + i\omega_{de}\right) \langle f_e \rangle_b = \langle C \rangle_b \left(\langle f_e \rangle_b - \langle \Phi \rangle_b\right) + iF_e(\omega_{de} - \omega_{*e}^T) \langle \Phi \rangle_b . \tag{3.19}$$

The nonlinear term has been absorbed in the total time derivative $d/dt = \partial/\partial t + \hat{\mathbf{b}} \times \langle \Phi \rangle_b \cdot \nabla$, and Φ has been normalized to e/T_e.

Before taking moments of this equation, let us calculate the total electron density, which we break into separate integrals over passing and trapped particles. Since the passing particles are adiabatic:

$$\begin{aligned} n_e(x,y,z) &= \int_p d^3v \Phi F_e + \int_t d^3v f_e \\ &= \int_p d^3v \Phi F_e + \int_t d^3v \left(\langle f_e \rangle_b - \langle \Phi \rangle_b F_e + \Phi F_e\right) \end{aligned}$$

The last line made use of Eq. (3.18). The adiabatic pieces for trapped and passing particles can now be combined:

$$n_e(x,y,z) = n_0 \Phi + \int_t d^3v \left(\langle f_e \rangle_b - \langle \Phi \rangle_b F_e\right). \tag{3.20}$$

As in the purely adiabatic limit, special treatment is required for components which are constant on flux surfaces, i.e. with $k_y = 0$. Treatment of this subtlety is postponed until Section 3.5. The velocity space integral over trapped particles in v and κ variables is

$$\int_t d^3v \, \langle f_e \rangle_b = \int_0^\infty 4\pi dv\, v^2 \int_{\sin(\theta/2)}^1 \frac{2B\epsilon_B \kappa \, \langle f_e \rangle_b \, d\kappa}{B_{\min}\sqrt{1-(B/B_{\min})(1-2\epsilon_B\kappa^2)}}, \tag{3.21}$$

where the κ integral is limited to the range $\sin(\theta/2)$ to 1, since at a given θ, only particles with turning points beyond θ will contribute to the local density, and $\kappa = \sin(\theta_t/2)$. Expanding for small ϵ, this takes the more familiar form:

$$\int_t d^3v \, \langle f_e \rangle_b = \sqrt{2\epsilon} \int_0^\infty 4\pi dv\, v^2 \int_{\sin(\theta/2)}^1 \frac{d\kappa\, \kappa \, \langle f_e \rangle_b}{\sqrt{\kappa^2 - \sin^2(\theta/2)}}.$$

We introduce the following shorthand notation for the pitch angle integration:

$$\langle A(\kappa) \rangle_\kappa = \int_{\sin(\theta/2)}^1 \frac{2B\epsilon_B \kappa A(\kappa) d\kappa}{B_{\min}\sqrt{1-(B/B_{\min})(1-2\epsilon_B\kappa^2)}}. \tag{3.22}$$

Averaging in pitch angle turns functions of κ into functions of θ, because of the θ dependence of the Jacobian and the turning points. The electron density in real space is just the κ average of the v-averaged $\langle f_e \rangle_b$. Defining a pitch angle dependent trapped electron "density" by integrating only over v:

$$n_t(x, y, \kappa) = \int_0^\infty 4\pi dv\, v^2 \, \langle f_e \rangle_b \, ,$$

the total electron density in real space is:

$$n_e(x, y, z) = n_0 \Phi + \langle n_t(x, y, \kappa) \rangle_\kappa - n_0 \langle \langle \Phi \rangle_b \, (x, y, \kappa) \rangle_\kappa. \tag{3.23}$$

The κ average of $\langle \Phi \rangle_b$ which appears here is analogous to the polarization density in the ion real space density, Eq. (2.9), and comes from the z-dependent part of the total electron distribution function.

3.2 Bounce Averaged Fluid Equations

As seen in the previous section, the pitch angle dependence of the electron distribution function enters the kinetic equation in a fundamentally different way than the v dependence. Firstly, the κ dependence of the toroidal precession drift is separable from the v dependence, and secondly, the bounce averaged potential which enters the kinetic equation is pitch angle dependent, since deeply trapped particles only respond to the potential on the outer midplane, while barely trapped particles respond to the potential averaged over the entire poloidal angle. This suggests a significantly different approach for deriving trapped electron fluid equations. For the ions, we take moments over $v_\parallel$ and $v_\perp$ of the five dimensional $f_i(x, y, z, v_\parallel, v_\perp)$ to obtain three dimensional ion fluid equations. For the electrons, we start with the five dimensional $f_e(x, y, z, v, \kappa)$ and bounce average, which removes the parallel coordinate. Then we only need to take moments over v of $\langle f_e \rangle_b (x, y, v, \kappa)$ to obtain three dimensional pitch angle dependent "fluid" equations for the electrons, which are functions of x, y, and κ. These moments can be thought of as the electron density, pressure, etc., of banana tips, since κ is directly related to the turning point by $\kappa = \sin(\theta_t/2)$. The resulting trapped electron fluid equations look similar to the 3D fluid equations derived in Chapter 2, with the parallel coordinate replaced by the pitch angle variable, κ. Retaining the pitch angle dependence of the electron moments allows us to keep the full pitch angle pitch angle dependence of the toroidal precession frequency and the bounce averaged potential. It also allows the use of a full pitch angle scattering Lorentz collision operator for electron collisions. When the real space electron density is needed in the quasineutrality constraint, we perform the κ average in Eq. (3.22).

We derive trapped electron moment equations by averaging in v over the bounce averaged electron distribution function, $\langle f_e \rangle_b$. Since only even powers of v appear in Eq. (3.19), we will only need even moments:

$$\begin{aligned}
n_t(x, y, \kappa) &= \frac{4\pi}{n_0} \int_0^\infty dv\, v^2 \langle f_e \rangle_b \,, \\
p_t(x, y, \kappa) &= \frac{4\pi}{3 n_0 v_{te}^2} \int_0^\infty dv\, v^4 \langle f_e \rangle_b \,, \\
r_t(x, y, \kappa) &= \frac{4\pi}{15 n_0 v_{te}^4} \int_0^\infty dv\, v^6 \langle f_e \rangle_b \,, \\
t_t(x, y, \kappa) &= \frac{4\pi}{105 n_0 v_{te}^6} \int_0^\infty dv\, v^8 \langle f_e \rangle_b \,, \\
v_t(x, y, \kappa) &= \frac{4\pi}{945 n_0 v_{te}^8} \int_0^\infty dv\, v^{10} \langle f_e \rangle_b \,,
\end{aligned}$$

where the electron moments have been normalized to their Maxwellian values. The

v^2 dependence of the bounce averaged precession frequency, Eq. (3.15), brings the next higher even moment into each dynamical equation, introducing the usual closure problem of the coupled moments hierarchy. Performing the v integration, we have:

$$\frac{dn_t}{dt} + \frac{3}{2}i\omega_{de}p_t - \frac{3}{2}i\omega_{de}\left\langle\Phi\right\rangle_b + i\omega_{*e}\left\langle\Phi\right\rangle_b = \left\langle C\right\rangle_b(n_t - \left\langle\Phi\right\rangle_b) \tag{3.24}$$

$$\frac{dp_t}{dt} + \frac{5}{2}i\omega_{de}r_t - \frac{5}{2}i\omega_{de}\left\langle\Phi\right\rangle_b + i(1+\eta_e)\omega_{*e}\left\langle\Phi\right\rangle_b = \left\langle C\right\rangle_b(p_t - \left\langle\Phi\right\rangle_b) \tag{3.25}$$

$$\frac{dr_t}{dt} + \frac{7}{2}i\omega_{de}t_t - \frac{7}{2}i\omega_{de}\left\langle\Phi\right\rangle_b + i(1+2\eta_e)\omega_{*e}\left\langle\Phi\right\rangle_b = \left\langle C\right\rangle_b(r_t - \left\langle\Phi\right\rangle_b) \tag{3.26}$$

$$\frac{dt_t}{dt} + \frac{9}{2}i\omega_{de}v_t - \frac{9}{2}i\omega_{de}\left\langle\Phi\right\rangle_b + i(1+3\eta_e)\omega_{*e}\left\langle\Phi\right\rangle_b = \left\langle C\right\rangle_b(r_t - \left\langle\Phi\right\rangle_b) \tag{3.27}$$

The collision terms will be discussed in Section 3.4. We require a closure approximation for the highest moment which models toroidal precession drift phase mixing. By analogy with Chapter 2, we use an extension of the method of [Hammett and Perkins, 1990]. For a 3-moment electron model (evolving n_t, p_t, and r_t) we choose:

$$t_t = -i\frac{|\omega_{de}|}{\omega_{de}}(\nu_a n_t + \nu_b p_t + \nu_c r_t), \tag{3.28}$$

and in the 4-moment electron model (also evolving t_t), we choose:

$$v_t = -i\frac{|\omega_{de}|}{\omega_{de}}(\nu_a n_t + \nu_b p_t + \nu_c r_t + \nu_d t_t). \tag{3.29}$$

As in Chapter 2, each closure coefficient has both a dissipative and non-dissipative piece, $\nu = \nu_r + i\nu_i|\omega_{de}|/\omega_{de}$, but now ω_{de} is pitch angle dependent. We choose these closure coefficients to closely approximate the bounce averaged kinetic response function, derived in the next section.

3.3 Electron Closures

From the linearized bounce kinetic equation, we can derive the response function for the pitch angle dependent electron density:

$$R_e = \frac{n_t(\kappa)}{n_0\, e\left\langle\Phi\right\rangle_b(\kappa)/T_e} = 4\pi\int dv\, v^2 F_e\frac{-\omega_{de} + \omega_{*e}^T}{\omega - \omega_{de}}, \tag{3.30}$$

which can again be factored into the form:

$$R_e = R_{e0} + \frac{\omega_{*e}}{\omega_{de}} R_{e1} + \frac{\omega_{*e}\eta_e}{\omega_{de}} R_{e2}. \tag{3.31}$$

These integrals can be performed analytically, and are functions of $x_e = \omega/\omega_{de}$ and κ (through $\omega_{de}(\kappa)$) [Tang, 1974].

$$R_{e0} = 1 + 2x_e + 2x_e^{3/2} Z(\sqrt{x_e}), \tag{3.32}$$

$$R_{e1} = -2[1 + \sqrt{x_e} Z(\sqrt{x_e})], \tag{3.33}$$

$$R_{e2} = -[1 + 2x_e + 2x_e^{3/2} Z(\sqrt{x_e})] + 3[1 + \sqrt{x_e} Z(\sqrt{x_e})], \tag{3.34}$$

where Z is the usual plasma dispersion function.

Choosing $\omega_{de} > 0$ to simplify the notation in the following expressions, the response functions from the 3-moment electron equations are:

$$R_{e0} = -\frac{12\,x_e^2 - 42\,\nu_c x_e - 105\,\nu_b + 30\,x_e - 105\,\nu_c + 105}{8\,x_e^3 - 28\,\nu_c x_e^2 - 70\,\nu_b x_e - 105\,\nu_a}, \tag{3.35}$$

$$R_{e1} = \frac{8x_e^2 - 28\nu_c x_e - 70\nu_b + 12x_e - 42\nu_c + 30}{8x_e^3 - 28\nu_c x_e^2 - 70\nu_b x_e - 105\nu_a}, \tag{3.36}$$

$$R_{e2} = \frac{12x_e - 42\nu_c + 60}{8x_e^3 - 28\nu_c x_e^2 - 70\nu_b x_e - 105\nu_a}, \tag{3.37}$$

and for the 4-moment electron equations:

$$R_{e0} = \frac{24x_e^3 - 108\nu_d x_e^2 - 378\nu_c x_e - 945(\nu_b + \nu_c + \nu_d - 1) + 60x_e^2 - 270\nu_d x_e + 210x_e}{-16x_e^4 + 72\nu_d x_e^3 + 252\nu_c x_e^2 + 630\nu_b x_e + 945\nu_a}, \tag{3.38}$$

$$R_{e1} = \frac{16x_e^3 - 72\nu_d x_e^2 - 252\nu_c x_e - 630\nu_b + 24x_e^2 - 108\nu_d x_e - 378\nu_c + 60x_e - 270\nu_d + 210}{16x_e^4 - 72\nu_d x_e^3 - 252\nu_c x_e^2 - 630\nu_b x_e - 945\nu_a}, \tag{3.39}$$

$$R_{e2} = \frac{-24x_e^2 + 108\nu_d x_e + 378\nu_c - 120x_e + 540\nu_d - 630}{-16x_e^4 + 72\nu_d x_e^3 + 252\nu_c x_e^2 + 630\nu_b x_e + 945\nu_a}. \tag{3.40}$$

Powell's method [Press *et al.*, 1986] is again used to determine the closure coefficients by minimizing the error between the fluid and kinetic response functions, R_{e0}, R_{e1}, and R_{e2}, along the real x_e axis for $-3 < x_e < 8$. The best fits are $\nu_a = (-.071, -.290)$, $\nu_b = (-.689, 1.102)$, and $\nu_c = (1.774, -.817)$ for the 3-moment model, and $\nu_a = (.073, .038)$, $\nu_b = (-.060, -.657)$, $\nu_c = (-1.085, 1.522)$, and $\nu_d = (2.073, -.905)$ for the 4-moment model. The response functions for the 4-moment model are shown in Fig. 3.2.

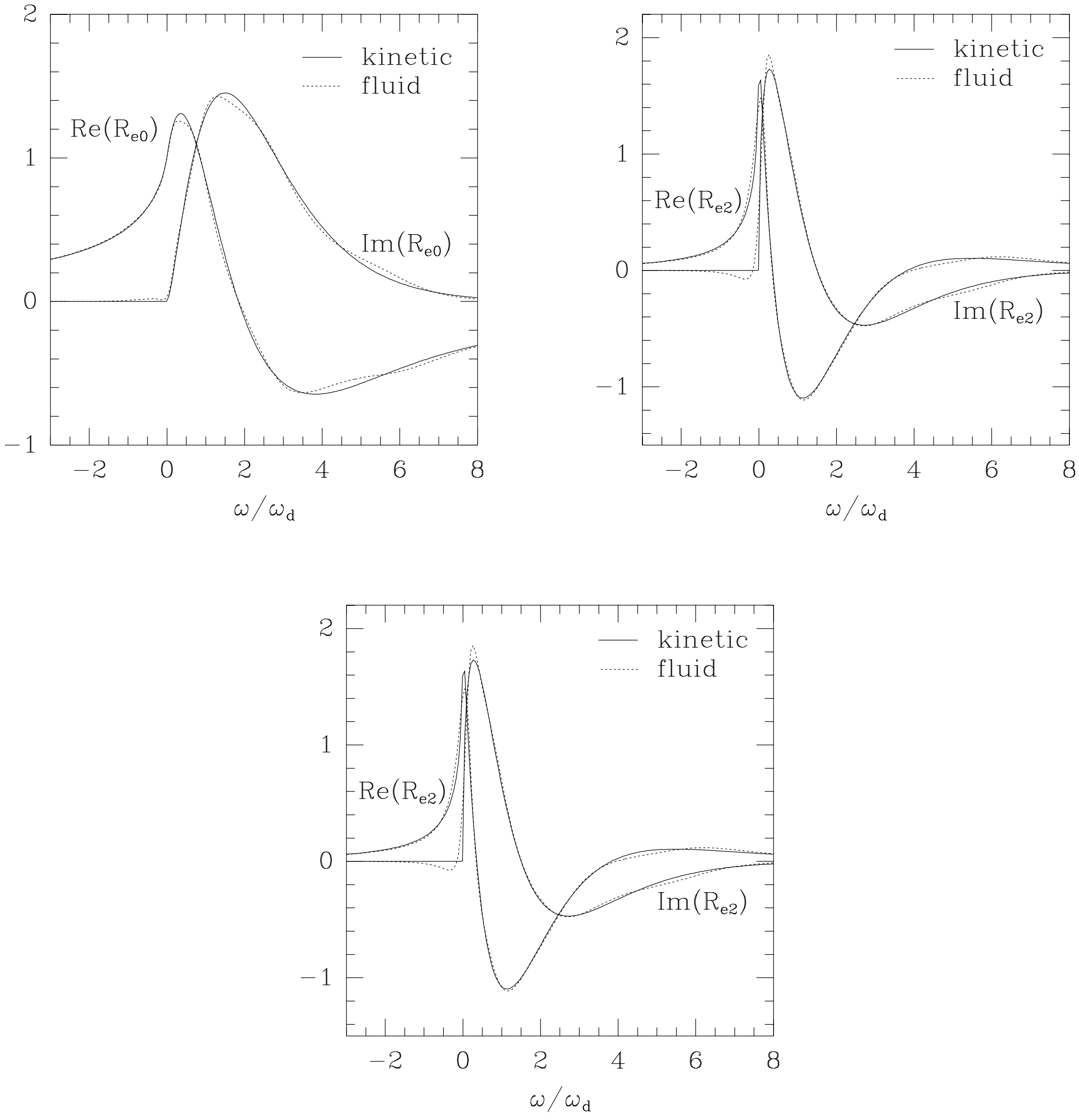

Figure 3.2: Kinetic and fluid bounce averaged response functions, R_{e0}, R_{e1}, and R_{e2}, for the 4-moment electron model.

3.4 Bounce Averaged Lorentz Collision Operator

Since the pitch angle dependence is retained in the trapped electron fluid moments, it is possible to use a Lorentz collision operator (a differential operator rather than a Krook algebraic model) for pitch angle scattering by electron-electron and electron-ion collisions:

$$C = \frac{\nu_e(v)}{2}\frac{\partial}{\partial\xi}(1-\xi^2)\frac{\partial f_e}{\partial\xi}, \tag{3.41}$$

where the pitch angle, $\xi = v_\parallel/v$. The energy dependent collision frequency is:

$$\nu_e(v) = \frac{4\pi n_e e^4 \ln\Lambda}{m_e^2 v^3}(Z_{\rm eff} + H_{ee}(v/v_{te})), \tag{3.42}$$

where the $Z_{\rm eff}$ part accounts for electron-ion collisions (assuming $v \gg v_{ti}$) summed over ion species ($Z_{\rm eff} = \sum_j Z_j^2 n_j/n_e$), and the $H_{ee}(x)$ part is from electron-electron collisions, where $H_{ee}(x) = \sqrt{2/\pi}\exp(-x^2/2)/x + [1-1/(x^2)]\mathrm{erf}(x/\sqrt{2})$. This collision operator conserves particles and energy, but not momentum. Electron-ion collisions do cause a loss of electron momentum, which is transferred to ion momentum, but is usually ignorable since $m_e \ll m_i$.

The bounce average of this collision operator enters Eq. (3.19), and is calculated in [Cordey, 1976; Hammett, 1986]:

$$\langle C\rangle_b = \frac{\nu_e}{2|\xi_0|\tau_b}\frac{\partial}{\partial\xi_0}\left[(1-\xi_0^2)\frac{\tau_b}{|\xi_0|}\left\{\left\langle\frac{B_{\rm min}}{B}\right\rangle_b - (1-\xi_0^2)\right\}\frac{\partial f}{\partial\xi_0}\right], \tag{3.43}$$

where ξ_0 is $v_\parallel/v$ at the midplane, $\xi_0 = \sqrt{1-\mu B_{\rm min}/E}$. Transforming to κ using $\xi_0 = \sqrt{2\epsilon_B}\kappa$, using Eq. (3.18) for f_e, and the fact that the adiabatic piece $F_e e\Phi/T_e$ is independent of pitch angle, we have:

$$\langle C\rangle_b = \frac{\nu_e}{8\epsilon_B^2|\kappa|\tau_b}\frac{\partial}{\partial\kappa}\left[(1-2\epsilon_B\kappa^2)\frac{\tau_b}{|\kappa|}\left\{\left\langle\frac{B_{\rm min}}{B}\right\rangle_b - 1 + 2\epsilon_B\kappa^2\right\}\times\right. \tag{3.44}$$

$$\left.\frac{\partial}{\partial\kappa}\left(\langle f_e\rangle_b - \langle\Phi\rangle_b\right)\right],$$

This collision operator must be integrated over velocity, v, to find the collision terms in the trapped electron fluid equations. This leads to two complications: the $1/v^3$ dependence of the electron-ion term is singular in the electron density equation, and the other integrals do not lead to simple combinations of the electron moments we evolve. For example, the collision term in the trapped electron pressure equation couples different moments together:

$$\frac{\partial p_t}{\partial t} = -\frac{4\pi}{3n_0 v_{te}^2}\int_0^\infty dv\, v^4 \left\langle C\right\rangle_b \propto -\nu_{e0}\int dv\, v \left\langle f_e\right\rangle_b \tag{3.45}$$
$$\propto -\nu_{e0}(\alpha n_t + \beta p_t + \cdots),$$

where in the last step, $\left\langle f_e\right\rangle_b$ has been expanded using the electron moments as a basis set, with as yet undetermined coefficients. To avoid solving the closure problem again, at this point we assume $\nu_e =$ constant, using:

$$\nu_e \approx \nu_{e0} = \frac{4\sqrt{2\pi} n_e e^4 \ln\Lambda}{3m_e^{1/2} T_e^{3/2}}(Z_{\rm eff}+1). \tag{3.46}$$

Integration over v then leads to the collision terms in Eqs. (3.24-3.27). A better approximation, which we leave to future work, would lead to weaker coefficients in the higher moment equations to model the velocity dependence of ν_e, but the present approximation captures the essential feature of the collision operator, which is primarily the pitch angle scattering process.

3.5 Evolution of Trapped Electron Moments

This section describes how these electron moment equations are solved. The emphasis is on numerical solution, but analytic solution would follow conceptually similar procedures.

In the numerical simulations described in later chapters, the ion gyrofluid moments are stored and evolved in (x, y, z) space. The parallel grid points are evenly spaced in $z = \theta$ from $-N\pi$ to $N\pi$, where $N \geq 1$, as discussed in Chapter 4. This parallel coordinate is linearly equivalent to the extended poloidal angle in the ballooning representation. The electron moments are stored and evolved in (x, y, κ) space. The pitch angle grid points are at $\kappa = \sin(\theta)/2$ to provide more resolution near the trapped-passing boundary where ω_{de} is varying rapidly. Separate electron moments are independently evolved in each magnetic well along the parallel coordinate, i.e., the moments for $-\pi < \theta < \pi$ are separate from the moments for $\pi < \theta < 3\pi$. The bounce averaged $\left\langle\Phi\right\rangle_b(x, y, \kappa)$ is calculated from $\Phi(x, y, z)$ by numerically integrating Eq. (3.12), and then used to advance the electron moments in time. Special care must be taken at the turning points, where Eq. (3.12) has integrable singularities. Choosing the κ spacing $\kappa = \sin(\theta/2)$ so that the turning points lie exactly on a θ grid point simplifies this integration. The electron nonlinearities are evaluated in a manner completely analogous to the ion nonlinearities, but in κ rather than in z. The electron collision terms are evaluated implicitly. The κ dependence in Eq. (3.44) and the boundary condition that $\langle f_e\rangle_b = \langle\Phi\rangle_b$ at the trapped-passing boundary automatically incorporates the strong effects of pitch angle scattering near the trapped-passing boundary.

Only the electron density moment ever needs to be evaluated in real space. To solve the quasineutrality equation, Eq. (2.9), the real space electron density, $n_e(x, y, z)$, is calculated by performing the κ averages of $n_t(x, y, \kappa)$ and $\langle\Phi\rangle_b$ as given by Eqs. (3.22) and (3.23). Again, special care must be taken at the turning points where Eq. (3.22) contains integrable singularities. Then the quasineutrality equation is solved for Φ, and this entire process is repeated for the next time step.

As in the adiabatic limit, special treatment is required for perturbations with $k_y = 0$, which are constant on flux surfaces. When $k_y \neq 0$, trapped electrons scattered onto passing orbits quickly become adiabatic, but this is not true if $k_y = 0$. When $k_y = 0$, $\omega_{de} = \omega_{*e} = 0$, so the bounce averaged kinetic equation reduces to:

$$\frac{d}{dt}\langle f_e\rangle_b = \langle C\rangle_b\left(\langle f_e\rangle_b - \langle\Phi\rangle_b\right). \tag{3.47}$$

The $k_y = 0$ electron moments for passing particles are separately evolved, and interact with the trapped electron $k_y = 0$ moments through collisions. We need to extend the κ variable to include passing particles, which occupy the range $1 < \kappa < 1/\sqrt{2\epsilon_B}$, and extend the definition of the bounce average for $\kappa > 1$:

$$\langle\Phi\rangle_b = \frac{\int_{-\pi}^{\pi} dz\,\Phi(x, z)/|v_\parallel|}{\int_{-\pi}^{\pi} dz/|v_\parallel|}, \tag{3.48}$$

for modes which are independent of y. For modes with $k_y \neq 0$, $\langle\Phi\rangle_b = 0$ for passing particles. Including nonadiabatic passing particles for $k_y = 0$, the generalization of Eq. (3.23) is:

$$n_e(x, y, z) = \int_p d^3v\, f_e + \int_t d^3v\, f_e = \int d^3v\left(\langle f_e\rangle_b - \langle\Phi\rangle_b F_e + \Phi F_e\right), \tag{3.49}$$

which can be written in the same form as Eq. (3.23),

$$n_e(x, y, z) = n_0\Phi + \langle n_t\rangle_\kappa - n_0\langle\langle\Phi\rangle_b\rangle_\kappa, \tag{3.50}$$

if we extend the κ average to include passing particles:

$$\langle A(\kappa)\rangle_\kappa = \int_{\sin(\theta/2)}^{1/\sqrt{2\epsilon_B}} \frac{2B\epsilon_B\kappa A(\kappa)d\kappa}{B_{\min}\sqrt{1-(B/B_{\min})(1-2\epsilon_B\kappa^2)}}. \tag{3.51}$$

When $n_t = 0$, Eq. (3.50) becomes $n_e = n_0(\Phi - \langle\langle\Phi\rangle_b\rangle_\kappa)$. That this is the proper adiabatic density response, Eq. (2.98), can be seen by using the identity $\langle\langle\Phi\rangle_b\rangle_\kappa = \int dz\, \Phi(x,y,z)/B$.

3.6 Comparison with Linear Kinetic Theory

We first test these trapped electron fluid equations by comparing the local linear growth rates and frequencies with kinetic theory. In the local limit, we choose $k_\| = 1/qR$, and ignore the bounce averages, i.e. we approximate $\Phi = \langle\Phi\rangle_b$. We also evaluate ω_{de} in the deeply trapped limit, at $\kappa = 0$. The local dispersion relation with trapped electrons is $R_i = -\tau R_e$, where the fluid and kinetic R_i's are given in Chapter 2 and the fluid and kinetic R_e's are given by Eq. (3.31) and Eq. (3.35)-(3.40). Fig. 3.3 shows the growth rates and real frequencies vs. $k_\theta\rho_i$ for the parameters $\eta_i = \eta_e = 3$, $q = 1.5$, $\epsilon_n = 1/3$, $\epsilon = 1/6$, and $T_i = T_e$, in the collisionless limit. The gyrofluid and trapped electron fluid results are in very good agreement with fully kinetic theory. The eigenfrequencies with adiabatic electrons are also shown. These are the same parameters as in Fig. 1 of [Kotschenreuther *et al.*, 1994b], and comparison with Fig. 3.4 shows that the destabilization by trapped electrons is strongly over-emphasized by the local and deeply trapped approximations, which neglect the bounce averaging of the potential and the variation of the toroidal precession frequency with pitch angle. Both of these effects will reduce the trapped electron density response. The three and four moment electron equations yield virtually identical results.

We next compare fully nonlocal results with kinetic theory in the collisionless limit. The eigenfrequencies from the six moment toroidal gyrofluid equations and the three moment trapped electron fluid equations are compared with fully kinetic calculations [Kotschenreuther *et al.*, 1994b] in Fig. 3.4. These results are for a pure deuterium plasma in the collisionless limit for the parameters $\eta_i = \eta_e = 3$, $\hat{s} = 1$, $q = 1.5$, $\epsilon_n = 1/3$, and $\epsilon = 1/6$, as in Fig. 1 of [Kotschenreuther *et al.*, 1994b]. The gyrofluid results with purely adiabatic electrons are also shown.

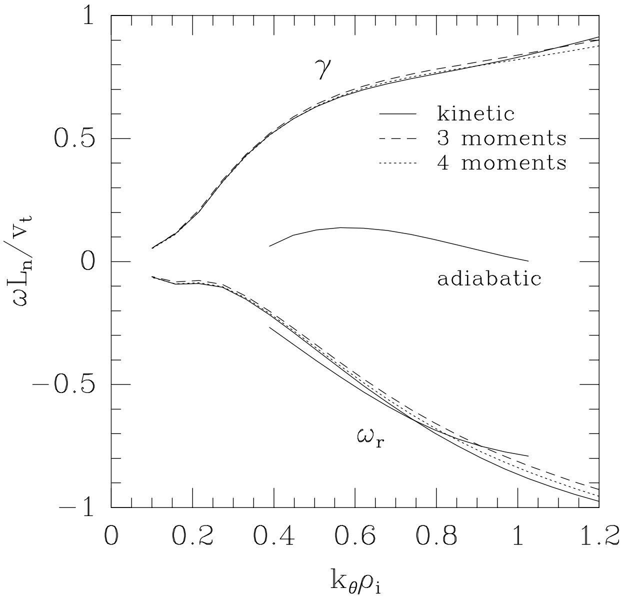

Figure 3.3: Comparison of local linear eigenfrequencies from gyrofluid and trapped electron fluid equations and fully kinetic results. The six moment toroidal gyrofluid equations are used, coupled with either the 3 moment or 4 moment electron equations. The fluid results are in very good agreement with kinetic theory. The results with adiabatic electrons are also shown. Comparison with Fig. 3.4 shows that the destabilization by trapped electrons is strongly over-emphasized by the local and deeply trapped approximations.

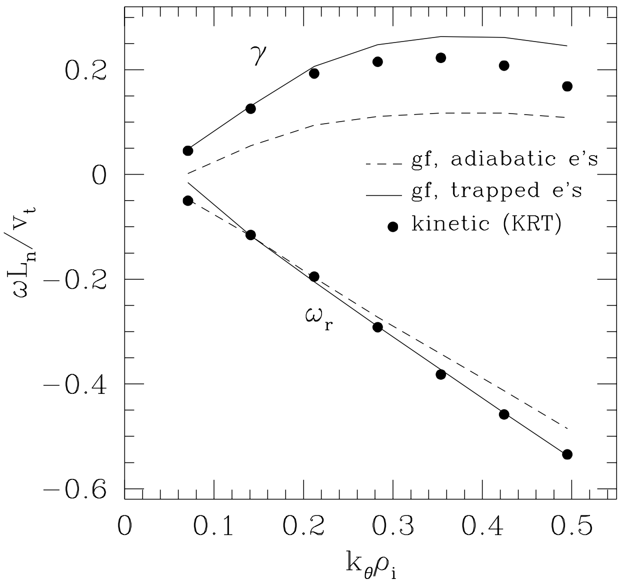

Figure 3.4: Comparison of linear eigenfrequencies from gyrofluid trapped electron fluid equations and fully kinetic results. The agreement is quite favorable. Also shown are the gyrofluid results with adiabatic electrons, showing that the trapped electron response doubles the growth rates for these parameters, even though this is an ITG mode.

The trapped electron response doubles the growth rates for these parameters, even though this is an ITG mode. Overall the agreement between gyrofluid and kinetic results is quite favorable.

Now we test our model of electron collisions by comparing with fully kinetic results. In Fig. 3.5, the variation of linear eigenfrequencies with collisionality is shown, for $k_\theta \rho_i = 0.35$, as in Fig. 2 of [Kotschenreuther *et al.*, 1994b]. The other parameters are as above. Again, there is very good agreement. The gyrofluid equations give a somewhat sharper transition from the collisionless regime to the strongly collisional regime where the electrons become adiabatic. Better agreement should be possible by modeling some of the velocity dependence of $\nu_e(v)$.

While trapped electrons have a strong effect on the ITG mode for low collisionality, the most interesting effect of the nonadiabatic electron dynamics is the destabilization of the trapped electron mode (TEM). For large collisionality the elec-

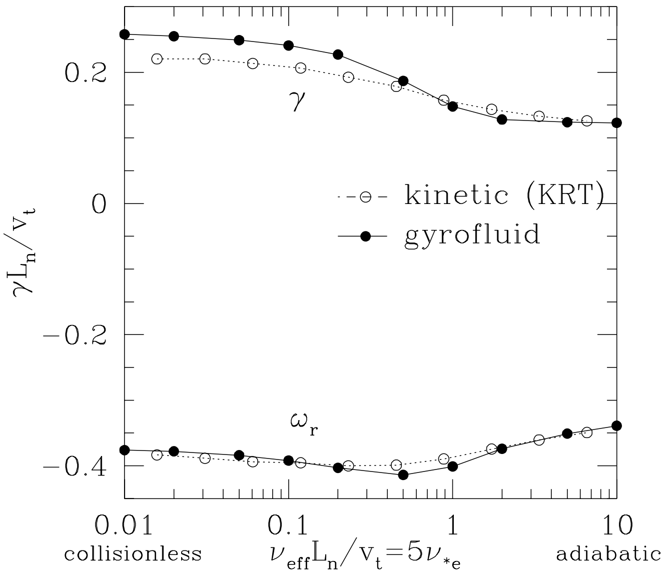

Figure 3.5: Variation of linear eigenfrequencies with ν_e, from kinetic theory and the gyrofluid trapped electron model. There is good agreement from the collisionless regime where the electron destabilization comes from the toroidal precession resonance, to the strongly collisional regime where the electrons become adiabatic.

trons are nearly adiabatic, and when η_i falls below a critical value, η_i^{crit}, the ITG mode is stabilized and the plasma is completely stable. At low collisionality, when η_i falls below the adiabatic η_i^{crit}, the trapped electron mode can still be unstable [Rewoldt and Tang, 1990]. Fig. 3.6 shows this behavior using the gyrofluid trapped electron model, for the parameters above, holding $\eta_i = \eta_e$. The solid squares are the linear growth rates for $k_\theta \rho_i = 0.3$ at large ν_{*e}. At this large collisionality, below $\eta_i \approx 1.5$, the ITG mode is stabilized. The open circles are the linear growth rates for $\nu_{*e} = 0.02$. For $\eta_i \gtrsim 1.5$, the ITG mode is unstable, and is further destabilized by trapped electrons (compared to its growth rate with adiabatic electrons). Below $\eta_i \approx 1.5$, it evolves into a trapped electron mode. When this transition occurs is a function of $k_\theta \rho_i$, so the trapped electron mode growth rates are also shown for $k_\theta \rho_i = 0.4$. Near $\eta_i = 1.5$, it is difficult to determine the eigenfrequency, since there are two unstable modes with nearly the same growth rates.

Thus, at low collisionality, the most striking effect of trapped electrons is to soften the ITG threshold. The TEM has quasilinear $Q_e > Q_i$, while the ITG mode has $Q_e < Q_i$, as in [Rewoldt and Tang, 1990], so the TEM can be expected to cause less ion heat transport. In this respect, there is still a threshold for the ion heat transport, but it is not a sharp threshold at low collisionality. Below the adiabatic ITG threshold, the growth rates become strong functions of electron collisionality and electron temperature and density gradients, which suggests that the turbulence levels and both ion and electron heat transport will be strongly dependent on these parameters in this regime.

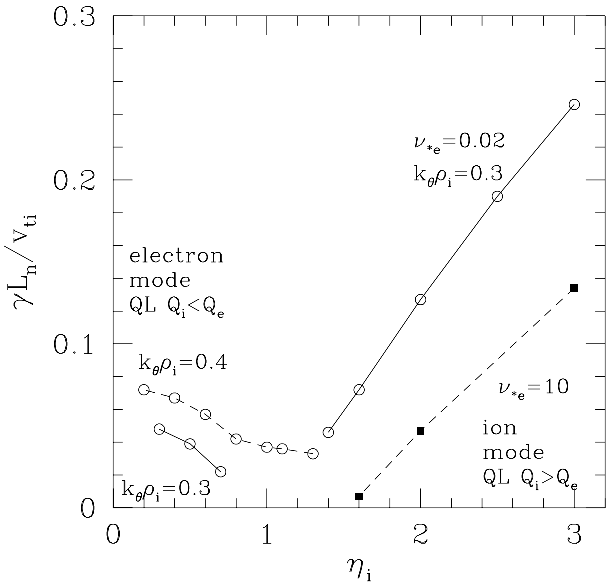

Figure 3.6: Linear growth rates from the gyrofluid trapped electron model varying η_i and holding $\eta_i = \eta_e$, showing the transition from an ITG mode to a trapped electron mode at $k_\theta \rho_i = 0.3$. At high collisionality (solid squares), $\nu_{*e} = 10$, the electrons are nearly adiabatic, and when $\eta_i \lesssim 1.5$ the plasma is completely stable. At low collisionality (open circles), $\nu_{*e} = 0.02$, for $\eta_i \lesssim 1.5$ the TEM is unstable. The TEM growth rate for $k_\theta \rho_i = 0.4$ is also shown, since the transition from ITG to TEM depends on $k_\theta \rho_i$.